

Analysis of Under-Actuated Snake Arm Robot

Xiaoqi Zhou, Feng Wang, Lei Dong and Zhongjian Dai
School of Automation, Beijing Institute of Technology, Beijing
ZXQ9283@163.com

Keywords: Snake arm robot, under-actuated structure, modeling analysis, error analysis.

Abstract : In view of the problem that traditional industrial robot can't adapt to some special areas due to its structural characteristics, a wire-driven snake arm robot, consisting of joints, drive mechanisms and a sliding rail platform is designed. In this paper, the structure characteristics of discrete series robot are analyzed in detail comparing with continuum robot. Moreover, the kinematic modeling of the under-actuated snake arm robot is established by using the method of continuum robot. Through simulation of the length of drawing wires, the relationships between the length of the wires and the bending angles and angles of joint rotation are obtained. The correctness and effectiveness of the robot are proved by analyzing and discussing the error factors of modeling and the attitude control experiments of the robot based on the space model.

1 INTRODUCTION

At present, when operation in some special fields and nonstructural environments, high requirements of robots for flexibility and the deformability to adapt to the environment are brought forward. Traditional robots fail to accomplish such work limited by size of joints and degrees of freedom (DOF), while continuum robots become a hot spot in recent research. Continuum robots achieves many developments and fruits by combining bionics, for instance, excellent compliance of elephant trunk robot or soft tentacle robot also shows the prospect and value of application of continuum robot in directions such as human-machine interface, grasping of complex fragile article and operation in confined space. On the other hand, however, infinite DOF of continuum robot brings the problems of difficulty in precise control, increasing of coupling and limited loading capacity resulting from insufficient rigidity. Comparatively, though compliance and DOF of discrete joints series manipulator decrease somewhat, its rigidity becomes better, and on the other hand, its discrete joints series construction increases the ability to locally control interested location. What's more, coordinates change between joints can control the spatial position of terminal actuator more accurately.

In fact, discrete serial construction is also embodied widely in biology field. The backbone

construction of vertebrate represented by snake is the discrete serial model which ensures both good rigid support and flexibility of movement due to hyper degrees of freedom resulting from multi joint series.

Both continuum and discrete multi joints robots have been studied and explored by many scholars at home and abroad. In paper (2010), Hu Haiyan et al. made analysis and description of mathematical model of a kind of continuum robots supported by flexible rod, and now the description of continuum robot kinematics in the literature adopts the method of correlating the drive space, workspace of the joints and operating space of the actuator which is accepted by most scholars. In recent years, some scholars start from bionics by focusing on description of movement mechanism of continuous body creature in the nature and attempt to find effective methods of movement control by imitating the movement models of continuous body creature. For example, paper (Cianchetti, 2011) to (Germán Sumbre, 2005) researched the motion mechanism of octopus tentacle, but the structure of the tentacles in the continuum form is simplified as piecewise discrete model which cannot effectively and truly restores the movement of natural organisms. For discrete serial construction, paper (G. Dogangil, 2010) proposed a method based on geometrically mirroring model for a kind of discrete under-actuated snake arm robot, calculating the relation between drive wires and the motion of joints,

coupling relation between every joint in detail, however, the process and calculation are too complex, and no effective experimental verification is given.

As mentioned above, continuum and discrete multi joints robots have their own advantages, but few literature analyzed ontology characteristics of discrete serial robot in depth and detail. With the discrete under-actuated snake arm robot as subject, this paper analyzes movement and structure features of this kind of robot in detail. Meanwhile by referencing the modeling of continuum robot, the kinematic model of the robot is established and the modeling error is analyzed. Finally an experiment is conducted to test modeling of discrete under-actuated snake arm robot and control the gesture of robot based on space model.

2 STRUCTURE CHARACTERISTICS OF UNDER-ACTUATED SNAKE ARM ROBOT

In some cases, operators hope to improve flexibility of motion of multi-joint robot to meet operational demand while not add actuators so that they don't have to increase the cost and power consumption of robot, and the introduction of under-actuated joints is a good solution to this contradiction. For description convenience, the wire-driven controlled joint is called active joint later in the paper, while the under-actuated joint is called driven joint. Under-actuated snake arm robot has two major advantages: firstly, compared to full drive construction, it can increase the compliance of local movement, the effect is shown in Fig. 1. The improvement of the local bending capacity is especially suitable for the operating requirements in confined spaces such as the detection of bent pipes.

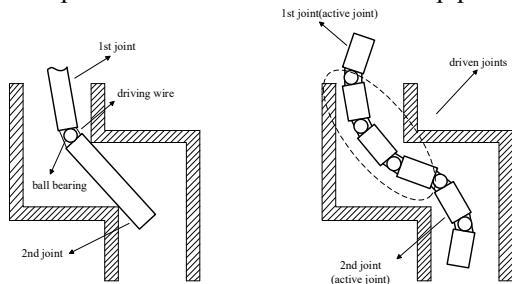


Figure 1. Performance comparison of under-drive structure

Secondly, the reconfiguration is enhanced. The driven joint can be added or removed flexibly within the controllable range of deformation. On one hand, effective operating length of robot can be changed

flexibly, on the other hand through combination of different numbers of driven joints in different region, different bending deformation can be generated to increase movement variation capability of interested location, as shown in Fig. 2.

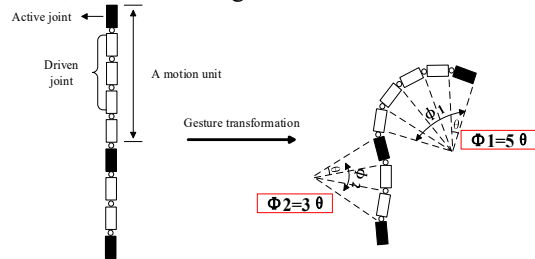


Figure 2. Reconfiguration of under-driven structure

Accordingly, within the range where degrees of freedom and the length of snake arm robot are controllable, through adding driven joints appropriately to form the under-actuated body, it can avoid adding actuators while improving movement compliance of the manipulator. It is an effective method to increase the operating capacity of joints series construction.

3 MECHANICAL STRUCTURE

The system of under-actuated snake arm robot is shown in Fig. 3, which includes snake arm joint, drive mechanism and slide movable platform.

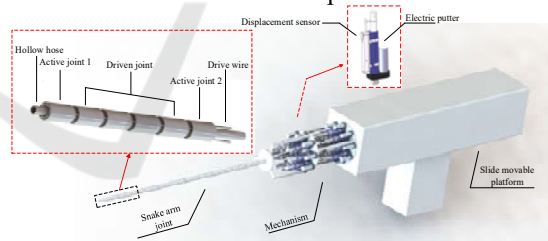


Figure 3. Under-actuated snake arm robot system

Drive mechanism of typical wire-driven is post positioned separated from the robot joints, only the drive wires or micro sensors are at the joint, and all drivers are integrated and put behind the joint body. On one hand, weight of robot joint can be reduced dramatically to ensure its flexibility of movement; secondly, long effective operating length or good loading capacity of robot can be ensured; and thirdly, when operating in high corrosion or dangerous environment, all electrical components don't contact internal operating environment directly, so the safety can be ensured. Drive device has many structures and realization forms, most of which are not fixed but

installed on movable platform. In addition to slide type shown in fig. 3, the movable platform can also be replaced with other types such as AGV, industrial robot. The mainly functioning of movable platform is to support movement of snake arm robot to realize large displacement of robot within certain space range, enabling the robot to reach working point quickly.

Drive mechanism consists of parallel joint actuators of snake arm robot, parallel arrangement of drivers simplifies the size of drive mechanism, reduces the coupling influence between every sub-driver. Thus the construction of serial joint and parallel drive is also one of structural features of such snake arm robot. Single joint driver consists of the electric putter with maximum thrust of 2,000N and displacement sensor.

Joint body consists of active joints, driven joints and ball bearings. Each group of motion unit includes one active joint and four driven joints which are connected through ball bearing, realizing spatial rotation. The joint and spherical are hollow construction, flexible hollow hose goes through the whole joint body forming the “framework” of robot, playing the role of support and limit setting.

Every active joint is driven by three wires distributing at even interval of 120°, and the driven joint is not driven directly by wire, and the wire hole of active joint distribution is shown in Fig. 4.

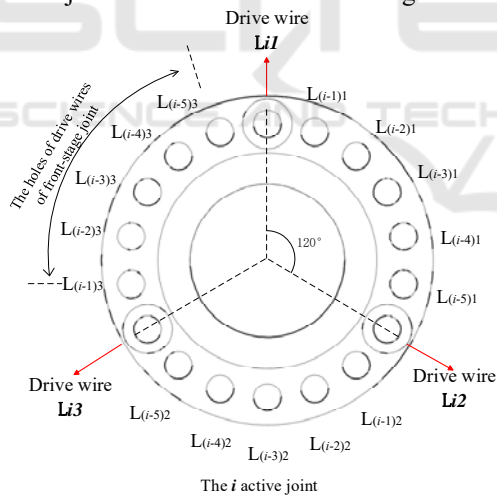


Figure 4. The schematic of hole distribution of the i -th active joint

Apparently, more rear the joint is at, more wires it will be passed through, because in addition to three wires driving current joint, wires of front every joint will pass through. In order to minimize coupling of movement between every joint, when the wires of front-stage joint reach concentric position of rear stage, they need to be arranged by staggering for certain angle for joints at adjacent stages.

4 MODELING ANALYSIS

Modeling of wire type under-actuated snake arm robot can reference the method of continuous robot. There are two reasons. First, adding a hollow hose in construction will make circuit easier to track. Besides, it also has function of elastic support and position restriction. This makes every part of robot joint move approximately to constant curvature bending as possible. In addition, by analyzing the morphology of robot at three different moments as shown in Fig. 5, it can be found that, at initial state a, all joint drive wires are in stretching state with physical feature of snake arm robot under discrete construction identical to that of continuum robot. Through state b to state c, the joint rotates to the maximum angle when the wire is at maximum bending. Infinitesimal method is used to make analysis of the movement, thus in unit time the model unit of discrete robot can be equivalent to continuum robot.

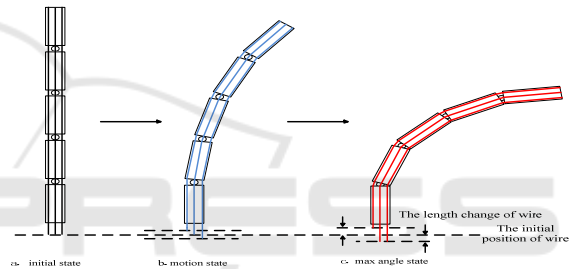


Figure 5. Three morphological changes of the snake arm robot

4.1 Kinematic Model

During movement of snake arm robot, bending angle θ and rotary angle Φ of a group of motion unit are realized by controlling the length of three pieces of evenly spaced drive wires of active joint. The operating space is shown in Fig. 6. If discrete joints of this group of motion unit are regarded as a section of continuous body, morphology variation of next group of motion unit driven by the wire is shown in Fig. 7.

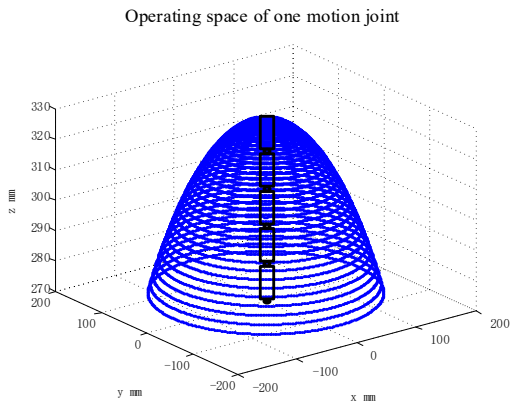


Figure 6. Operating space of one motion joint

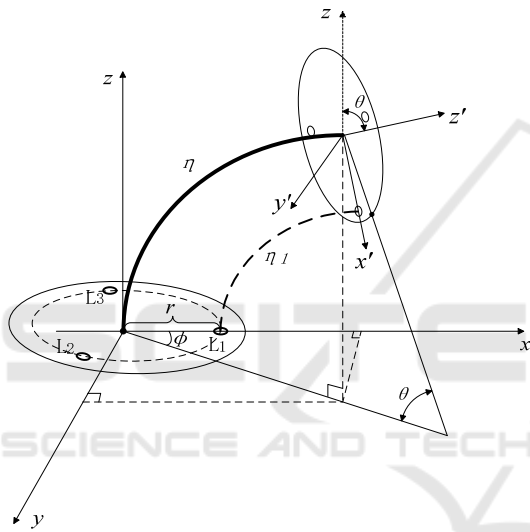


Figure 7. The attitude change of a set of motion unit under continuous form

Assuming that the original length of the three drive wires is l , and the length of motion units after driving are changed to l_1, l_2 and l_3 respectively, while length variation of drive wire is expressed as ΔL_i ($i=1,2,3$), and the circumference radius of the driving wire through hole is r (in this paper, $r=1.25\text{cm}$). From Fig. 7 the relation between ΔL_i and bending angle θ , rotary angle Φ is obtained as shown in equation 1 to 3, where θ is valued $[-30^\circ, 30^\circ]$, Φ is valued $[0^\circ, 360^\circ]$:

$$\Delta L_1 = l - l_1 = (\eta - \eta_1)\theta \cos \Phi = r\theta \cos \Phi \quad (1)$$

$$\Delta L_2 = l - l_2 = (\eta - \eta_2)\theta \cos\left(\Phi + \frac{2\pi}{3}\right) = r\theta \cos\left(\Phi + \frac{2\pi}{3}\right) \quad (2)$$

$$\Delta L_3 = l - l_3 = (\eta - \eta_3)\theta \cos\left(\Phi + \frac{4\pi}{3}\right) = r\theta \cos\left(\Phi + \frac{4\pi}{3}\right) \quad (3)$$

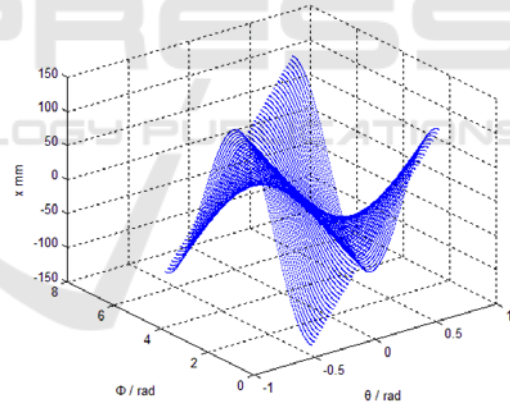
The relationship between the rotary angle Φ and the change of the wire length can be solved from (2) and (3):

$$\Phi = \arctan\left[\frac{\Delta L_2 - \Delta L_3}{\sqrt{3}(\Delta L_2 + \Delta L_3)}\right] \quad (4)$$

Within $[0, 2\pi]$, Φ will contain two solutions with a different value of π . If using x axis as starting axis, with counterclockwise direction as positive direction, it can be analyzed through equation (1) that when $\Delta L_1 < 0$, Φ takes the solution within $[\pi/2, 3\pi/2]$; when $\Delta L_1 > 0$, Φ takes the solution within $[0, \pi/2]$ or $(3\pi/2, 2\pi]$. Bending angle θ of motion unit can be obtained by the following equation:

$$\theta = \frac{\Delta L_1}{r \cos \Phi} \quad (5)$$

Through equation (1) to (5) we obtained the mapping relation between movement space and drive space of the joints, and the state of the other variable can be obtained through any variation of either known angle or known wire length. Through simulation the relation between variation of length L_1 of drive wire, bending angle and rotary angle is obtained as shown in Fig. 8.

 The relationship between the change of drive wire L_1 and the angles

 Figure 8. While $\theta = [-30^\circ, 30^\circ]$, $\Phi = [0^\circ, 360^\circ]$, the curve diagram of the length change of drive wire L_1

If keep rotary angle constant (in simulation with $\Phi=0^\circ$ as an example), when bending angle varies continuously, the relation between length variation of 3 wires is shown in Fig. 9. It is a linear variation with a certain slope. When bending angle keeps constant (in simulation with $\Phi=30^\circ$ as an example), when rotary angle varies continuously ($[0, 2\pi]$), the relation between length variation of 3 wires is shown in Fig. 10. When bending angle and rotary angle both vary continuously, by combining results of Fig. 9 and Fig.10 we can obtain the “isogonal line” (Fig. 11) of 3

drive wires. In the figure, a straight line drawn along any slope represents the relation between continuously varying bending angle and the variation of the wire under a given rotary angle. While the line is in different circular lines, it represents the relation between continuously varying rotary angle and the variation of the wire under a given bending angle.

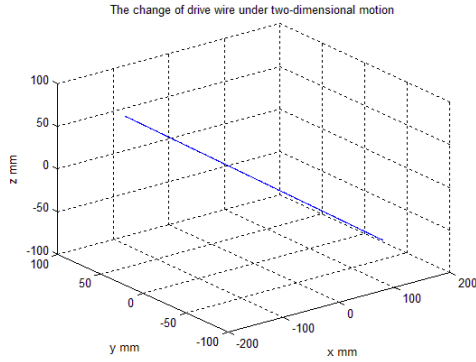


Figure 9. While $\Phi=0^\circ$, $\theta=[-30^\circ,30^\circ]$, the relationship of the length change of 3 drive wires

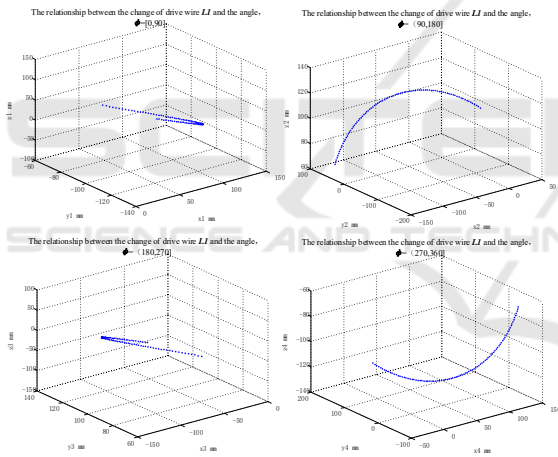


Figure 10. While $\theta=30^\circ$ $\Phi=[0^\circ,360^\circ]$, the relationship of the length change of 3 drive wires

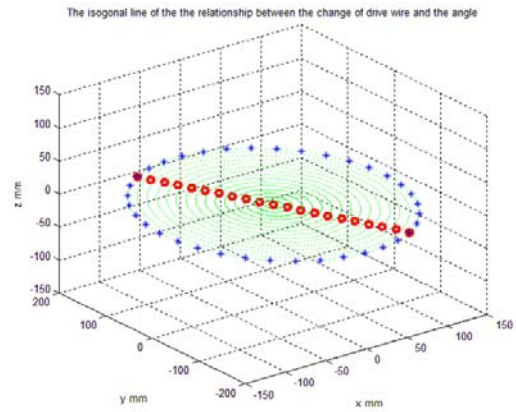


Figure 11. While $\theta=[-30^\circ,30^\circ]$ $\Phi=[0^\circ,360^\circ]$, the “isogonal line” relationship of the length change of 3 drive wires

In fact, because every group of motion unit consists of several serial joints, when we obtain the varied angle, we can more accurately subdivide the spatial position in a group of motion unit. In other words, compared to true continuous construction, more accurate spatial position of robot can be obtained under discrete series type construction. Because two adjacent joints are connected only through ball-joint without other link rod construction of unit length, coordinate transformation between two adjacent joints can be obtained only through rotation calculation. If the coordinate of snake arm robot base is defined, and the bending angle and rotary angle of robot are obtained, we can obtain the spatial position of any joint through matrix transformation between two adjacent joints. The rotation matrix between two adjacent joints is:

$$T_i = \begin{bmatrix} c^2\varphi c\theta + s^2\varphi & s\varphi c\varphi c\theta - s\varphi c\varphi & -s\theta c\varphi \\ s\varphi c\varphi c\theta - s\varphi c\varphi & s^2\varphi c\theta + c^2\varphi & -s\varphi s\theta \\ s\theta c\varphi & s\varphi s\theta & c\theta \end{bmatrix} \quad (6)$$

Where s stands for sin, c stands for cos, Φ is the rotation angle to the x-axis and the θ is the bending angle to z axis.

On the other hand, there will be mutual coupling in the movement of joints of snake arm robot, and the movement coupling originates from layer-by-layer superposition of drive wires. Namely, the drive wire of former stage (suppose that the first stage motion unit close to end-effector is set as stage 1) will always reach the drive mechanism through the latter stage joint. So, when driving the latter stage joint (for example, No. i stage motion unit), the drive wire of its No. i-1, i-2 ... till No. 1 section joint will be all influenced by coupling. We only need to analyze the coupling relation of wires when two adjacent stage active joints move, and the movement coupling of other more

stages of joints is only overlapping on the basis. Taking the movement unit of the $i-1$ and the i as examples, as shown in the figure12, the movement of stage $i-1$ motion unit does not influence stage i , but the movement of stage i motion unit can influence length variation of stage i -d wire, the angle difference of drive wire of two adjacent active joint concentric hole position is $\pi/9$, so when stage i motion unit acts, coupling variation of 3 stage $i-1$ drive wires is:

$$\begin{aligned}\Delta L'_{(i-1)1} &= r\theta_i \cos(\varphi_i + \pi/9) \\ \Delta L'_{(i-1)2} &= r\theta_i \cos(\varphi_i + 7\pi/9) \\ \Delta L'_{(i-1)3} &= r\theta_i \cos(\varphi_i + 13\pi/9)\end{aligned}\quad (7)$$

Consequently, when stage $i-1$ motion unit is driven, the length variation of its 3 drive wires shall overlay the coupling variation resulting from movement of stage i motion unit on the basis of their respective theoretical calculated value.

It is worth mentioning that using some effective control methods such as tip-following (the movement of the next level of motion unit follows the action of the previous one) can greatly reduce the movement coupling between motion units so as to improve the flexibility of movement.

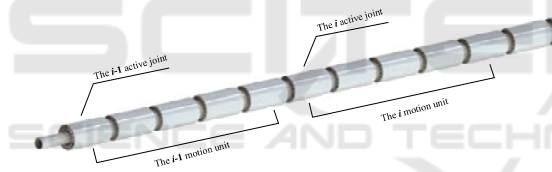


Figure 12. Two levels motion units

4.2 Model Error

The model error of the discrete under-actuated snake arm robot is mainly due to the fact that the driving cable is regarded as constant curvature when modeling, while the drive wire are typically in the form of multi-segment fold line in practice. So there is error between models of curve and fold line.

Assuming that at bending angle θ the drive wire of robot single joint section bends into a fold line consisting of n sections of straight line, as shown in the figure 13. And the length of every section of fold line can be obtained by the following equation:

$$s = 2 \sin\left(\frac{\beta}{2}\right) \cdot l' / \theta = 2 \sin\left(\frac{\theta}{2n}\right) \cdot l' / \theta \quad (8)$$

Where β is the bending angle corresponding to single section of fold line, l' is the arc length when the shape of drive wire bending is an ideal arc.

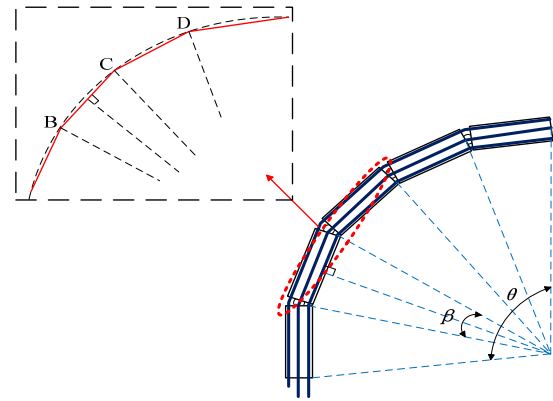


Figure 13. diagram of multiple poly lines

The total error of the length of a single drive line is derived from the following equation:

$$e = l' - \sum_{j=1}^n s_j = l' - n \cdot \left(2 \sin\left(\frac{\theta}{2n}\right) \cdot l' / \theta\right) = l' \left(1 - \frac{2n}{\theta} \cdot \sin\left(\frac{\theta}{2n}\right)\right) \quad (9)$$

In this paper, the snakelike robot has six sets of motion units, so the maximum number of broken lines is 30, and the maximum bending angle is π . In this case, there is a maximum error:

$$e_{\max} = l' \left(1 - \frac{60}{\pi} \cdot \sin\left(\frac{\pi}{60}\right)\right) = 0.007l' \quad (10)$$

From this we can see that, when we consider the drive line at back of the driven joint as arc of even curvature, the maximum error between the line length and the length of the actual multi segment line is about 7‰, and this error is within our acceptable range. Moreover, each joint of snakelike robot is controlled independently. Thus the error of wire will not accumulate. So it's valid to assume that the line between the two active joints is arc.

5 EXPERIMENTS AND RESULTS

Freescale DSP 56F8037 is adopted as the control chip in the arm robot. The displacement sensor of drive wire is KTC bar type electronic rule. The data collected by the displacement sensor are filtered by Kalman filter to remove the White Noise.

The displacement sensor is calibrated, and the length change of the displacement sensor and the measured data is shown in the table. Table 1 calibration data of displacement sensor.

Table 1. calibration data of displacement sensor

length /cm	AD sample mean	length /cm	AD sample mean
0	133	5	7544
0.5	612	5.5	8319
1	1432	6	9088
1.5	2216	6.5	9863
2	2976	7	10721
2.5	3711	7.5	11494
3	4442	8	12369
3.5	5209	8.5	13215
4	5977	9	14071
4.5	6754	9.5	15066

Starting from the initial 0cm, we recorded the filtered AD sampling value twice at each 0.5cm progressive of displacement sensor and got the average. The AD sampling difference of each 0.5cm is calculated respectively, then remove the value under initial length and the maximum length of the larger fluctuations, add the remaining AD difference and take the average, finally the relationship between the actual length variation of the displacement sensor and the sampling value of AD can be determined: for each change of 0.5cm, the change of AD sampling value is about 792.

For the control of the snake arm robot, the PI control law is adopted, and the control structure block diagram is shown in the figure 14.

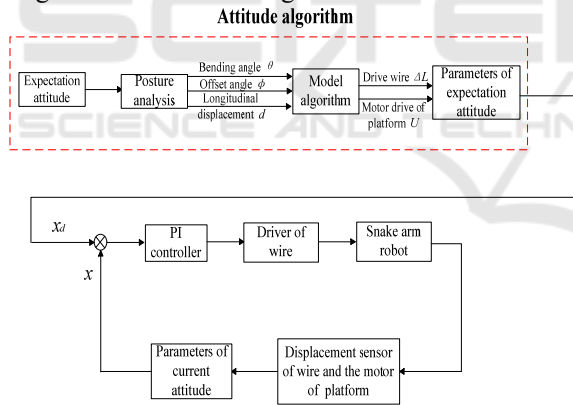


Figure 14. control structure of attitude control of snake arm robot

A set of motion units of the robot arm is measured experimentally, and the experimental results and the curves of the length of the drive wire are shown in the figure.

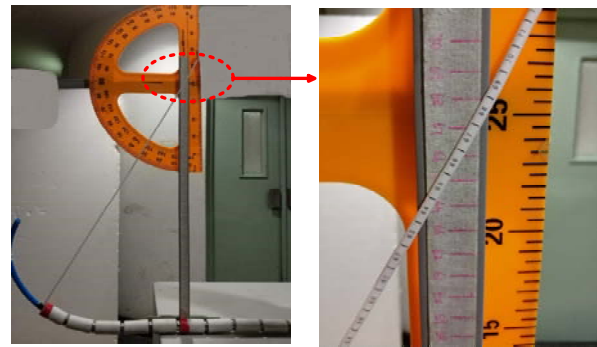


Figure 15. Mechanical arm 30 degree bending test

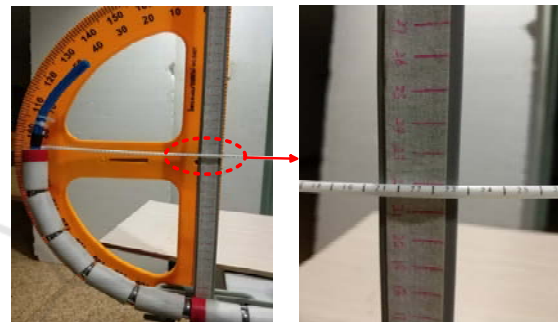


Figure 16. Mechanical arm 90 degree bending test

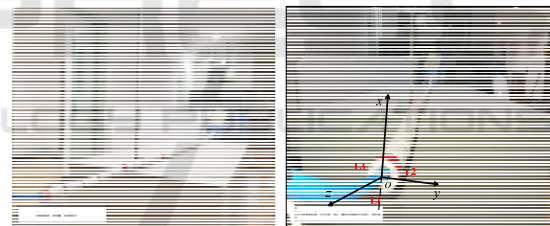


Figure 17. Manipulator coordinate

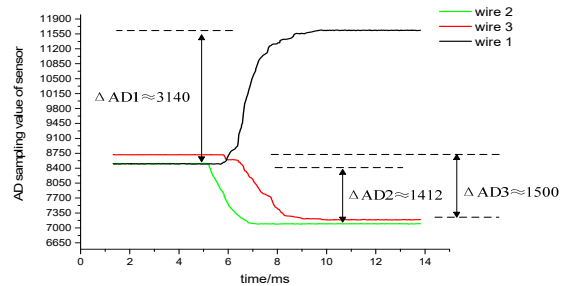


Figure 18. Change curves of driving lines when bending 90 degrees

When the bending is 90 degrees, according to the formula given in the previous paper, the theoretical calculation value of the length change of the three

driving wires is respectively: $\Delta L_1=1.96\text{cm}$, $\Delta L_2=\Delta L_3=-0.98\text{cm}$ (the reference coordinate system is shown in Figure 17). The change curves of actual length of driving wires are shown in Figure 18, and the errors of L1, L2, L3 are respectively 1%, 9.2%, 3.5%.

The control effects of S curve attitude and compliant bending attitude of manipulator is shown in this paper.



Figure 19. S curve attitude



Figure 20. Bending attitude

6 CONCLUSIONS

In this paper, we discussed and analyzed series snake arm robot with wire-driven, under-actuated and multi degrees of freedom under discrete structure. Specifically, the characteristics and differences of discrete joint snake arm manipulator, traditional rigid robot and continuum robot are analyzed, and the structural characteristics and application advantages of discrete robot are discussed. In addition, based on the modeling method of continuum robot, modeling analysis and error analysis of a ball-connected snake arm robot are carried out, and the "Isometric" change diagram relationship between the space angle and the drive wire of robot is obtained. Finally, through the closed-loop attitude control, the attitude and deflection angle of the snake arm robot are controlled effectively.

REFERENCES

HU Haiyan, WANG Pengfei, SUN Lining, ZHAO Bo, LI Mantian. Kinematic Analysis and Simulation for Wire-

- driven Continuum Robot [J]. JOURNAL OF MECHANICAL ENGINEERING, 2010, 46(19):1-8.
- Cianchetti, M., Arienti, A., Follador, M., Mazzolai, B., Dario, P., & Laschi, C. (2011). Design concept and validation of a robotic arm inspired by the octopus. *Materials Science & Engineering: C*, 31(6), 1230-1239.
- Kang, R., Branson, D. T., Guglielmino, E., & Caldwell, D. G. (2012). Dynamic modeling and control of an octopus inspired multiple continuum arm robot. *Computers & Mathematics With Applications*, 64(5), 1004-1016.
- relli M, Renda F, Calisti M, et al. Learning the inverse kinetics of an octopus-like manipulator in three-dimensional space. *Bioinspir Biomim*. 2015;10(3):035006.
- Germán Sumbre, Fiorito, G., Flash, T., & Hochner, B. (2005). *Neurobiology: Motion control of flexible octopus arms*. *Nature*, 433(7026), 595-596.
- G. Dogangil, B. Davies, F.R. y Baena. A review of medical robotics for minimally invasive soft tissue surgery *Proc. Ins. Mech. Eng. Part H*, 224 (5) (2010), pp. 653-679
- YUAN Wei, WEI Zhiqiang, ZOU Fang, YAO Yanbin. Kinematical Analysis of an Underactuated Snake arm Robot[J]. *Machinery&Electronics*, 2014, (11):65-67,68.
- Dong, X., Raffles, M., Guzman, S. C., Axinte, D., & Kell, J. (2014). Design and analysis of a family of snake arm robots connected by compliant joints. *Mechanism & Machine Theory*, 7773-91.
- Hannan MW, Walker ID. Kinematics and the implementation of an elephant's trunk manipulator and other continuum style robots. *J Robot Syst*. 2003 Feb;20(2) 45-63. PMID: 14983840.
- Zheng Li, Ruxu Du. Design and Analysis of a Bio-Inspired Wire-driven Multi-Section Flexible Robot. *International Journal of Advanced Robotic Systems* 2013 Vol.10 1729-8806.
- Laschi C., Mazzolai B., el. "Design of a biomimetic robotic octopus arm", *Bioinspiration & Biomimetics*, vol. 4, 2009 015006.
- Bajo A., and Simaan N., "Finding Lost Wrenches: Using Continuum Robots for Contact Detection and Estimation of Contact Location", 2010 IEEE International Conference on Robotics and Automation, Anchorage, Alaska, May, 2010, pp. 3666-3673
- Y.-J. Kim, S. Cheng, S. Kim, K. Iagnemma Design of a tubular snake arm manipulator with stiffening capability by layer jamming. 2012 IEEE/RSJ International Conference on Intelligent Robots and Systems, October 7-12, 2012, Vilamoura, Algarve, Portugal, IEEE (2012), pp. 4251-4256
- Li, Z., Ren, H., Chiu, P. Y., Du, R., & Yu, H. (2016). A novel constrained wire-driven flexible mechanism and its kinematic analysis. *Mechanism & Machine Theory*, 9559-75.
- R.J. Webster, B.A. Jones Design and kinematic modeling of constant curvature continuum robots: a review. *Int. J. Robot. Res.*, 000 (00) (2010), pp. 1-22
- Han Yuan, Zheng Li, Workspace analysis of wire-driven continuum manipulators based on static model, *Robotics and Computer-Integrated Manufacturing*, 2018, 49, 240

Z. Li, R. Du Design and analysis of a bio-inspired wire - driven multi-section flexible robot Int. J. Adv. Robot. Syst., 10 (209) (2013), pp. 1-11

Rongjie Kang, Emanuele Guglielmino, Letizia Zullo, David T Branson, Isuru Godage, Darwin G Caldwell, Embodiment design of soft continuum robots, Advances in Mechanical Engineering, 2016.

